


An acoustic method for condition classification of a water-filled underground siphon

Advances in Mechanical Engineering
2019, Vol. 11(4) 1–12
© The Author(s) 2019
DOI: 10.1177/1687814019840893
journals.sagepub.com/home/ade


Zao Feng¹ , Kirill V Horoshenkov² and GuoYong Huang¹

Abstract

This article reports on an application of the k-nearest neighbours pattern recognition and classification technique to condition monitoring in a full-scale, water-filled siphon that is located beneath the underground. An experimental facility has been designed and constructed at the University of Bradford to study using acoustic waves as excitation to observe the characteristics of pipe sediments and wall damages on an underground sewer siphon. The effects of different amounts of sediment inside the siphon and different size of artificial damage on the pipe wall have been studied. The sound pressure level and acoustic energy were calculated from the acoustic signals which were recorded from three hydrophones under several representative siphon conditions to extract useful features in order that the proposed k-nearest neighbours classification algorithm could be applied. It has been proven that acoustic-based approach is capable of providing sufficient information on the condition of pipes for reliable classification and fault detection.

Keywords

Acoustics, underground siphon, signal processing, pattern recognition

Date received: 11 January 2018; accepted: 6 March 2019

Handling Editor: Pietro Scandura

Introduction

Water distribution systems are key elements of urban water infrastructure. These systems are gradually deteriorating due to their ageing, operational stresses and external environmental conditions.¹ A majority of these assets are hidden underground so that they are difficult to access for routine visual inspection. As a result, there is a need for a robust, remote method of inspection that can be used to detect a critical change in order to optimise their maintenance costs, or ensure timely rehabilitation work.² For the inspection of water pipes, a few techniques have been developed and used in the field, for example, closed circuit television (CCTV) and laser scan are well-adopted visual inspection techniques which however are only operational above waterline.^{3,4} In addition, various geophysical techniques, such as ground penetrating radar (GPR) exist to assess the exterior of pipes.^{5,6} In recent years, there has been a

growing interest in using acoustic technologies for condition monitoring applications such as sonar profiling system, guided wave ultrasound and a number of multi-sensors systems are in development.^{7–9}

Sound waves can propagate through media which is inaccessible to light or electromagnetic radiation. These media include water filled drainage pipes in which the turbidity of water is too high to be able to use conventional CCTV inspection method.¹⁰ The frequency

¹Department of Information and Control Engineering, Kunming University of Science and Technology, Kunming, P.R. China

²The University of Sheffield, Sheffield, UK

Corresponding author:

GuoYong Huang, Department of Information and Control Engineering, Kunming University of Science and Technology, Jingming South Road, Chenggong, Kunming 650500, P.R. China.
Email: huanggy@nuaa.edu.cn



composition, temporal patterns and energy of the sound waves which propagate through a pipe are coloured by the structure conditions of the pipe walls, quality of the pipe joints, wall roughness and by the amount of sediment present in the pipe.¹¹ This information can be used directly, or after some conditioning, in the pattern classification process. In this process feature, extraction is a critical step as we desire to extract only those features representing the characteristics of this process by separating them from various unwanted disturbances. There are a large number of signal processing methods available to extract meaningful features from the recorded sounds, such as Short-Time Fourier Transform (STFT), Wavelet Transform (WT), Mel-Frequency Cepstral Coefficients (MFCCs) and Wigner-Ville Distribution (WVD).¹² Many of these methods have been developed and tested extensively condition classification with acoustic means through hidden Markov models (HMMs), k-nearest neighbours (KNN), decision trees or neural networks.¹³ Although these algorithms have been developed and applied successfully in areas like biometrics, no extensive applications were found in the condition monitoring of buried civil facilities.¹⁴ Therefore, it is important to study and reveal the patterns that represent particular condition states, and to discover the relation between acoustic features and a series of patterns labelled by a full-scale model of a hydraulic siphon.

In this analysis, the sound pressure level of the acoustic signals emitted in the siphon were analysed using the Schroeder integration method within a number of different frequency bands. The acoustic energy contained in each of the filter bands was then used as meaningful feature for condition classification. The acoustical signals used in analysis were collected from a hydrophone array. KNN classification method was then trained and applied to determine the structural and operational conditions in the siphon. Although there are many studies for general purpose of sound/speech recognition system in the literature, the

available water-filled acoustic signal recognition studies are limited. One example work developed in Yuan et al.¹⁵ using Tikhonov regularisation to establish the optimization objective function. In another study,¹⁶ acoustic signals were modelled by matched field processing in the frequency domain. The proposed KNN classification system is different from the other methodologies by acoustic energy and combines with KNN classifier, it is tested to be reliable under various pipe conditions including sediment and damage with pipe being surrounded by different medium.

Experimental methodology

Experiment setup

A 4.2 m long and 2.0 m high siphon using sections of 450 mm concrete pipes was installed on a 500 mm layer of fine sand in an open top box made of 12 mm plywood as shown in Figure 1. The siphon was filled up with clean water to the level of 900 mm below the top rims of the vertical parts, and the water level remained during all the experiments as reference. The siphon was instrumented with four 25 mm hydrophones (Type SQ31 by Sensor Technology Inc. Canada), hydrophone 1–hydrophone 3 were installed in the left leg of the siphon (The hydrophones are named with capital letter H followed by a number which is addressed to its position in the test rig in the following text). Hydrophone 4 was installed in the right leg of the siphon 30 mm above the speaker and used as a reference receiver as shown in Figure 2. The source was a 50 mm diameter water resistant speaker that was situated in a polyvinyl chloride (PVC) enclosure (Type K50WP by Visaton Germany). The speaker and three hydrophones were securely attached to two aluminium tubes and placed into the opposite legs of the siphon and kept at the same positions in all of the experiments conducted in the siphon. Figure 2 illustrates schematically the arrangement of this experiment.

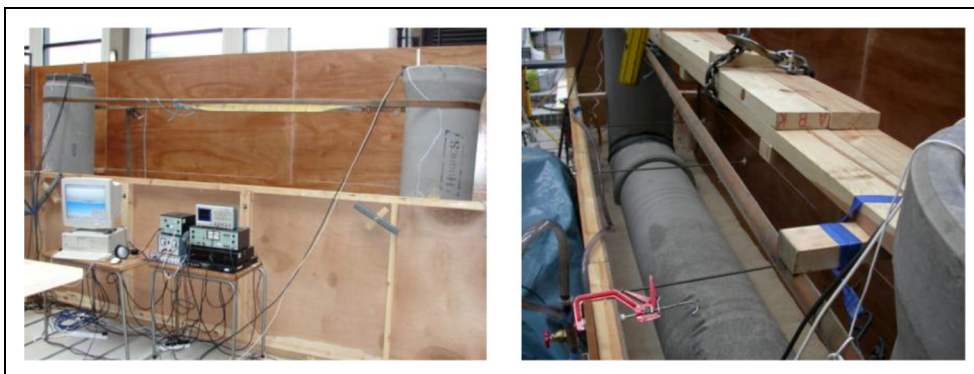


Figure 1. Experimental siphon constructed in the hydraulics laboratory at the University of Bradford.

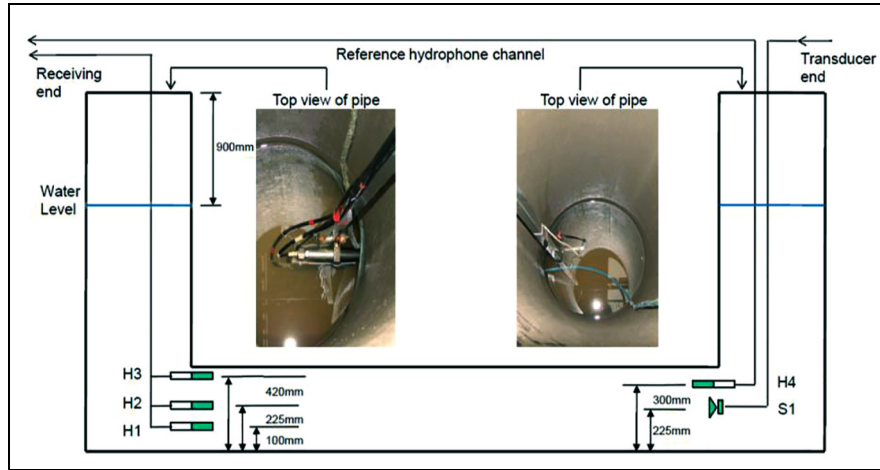


Figure 2. Structure of the siphon and acoustic sensors.

The data acquisition system consisted of the following: (1) a computer (with a sound card) installed with WinMLS software; (2) four 8-channel high-pass hydrophones, (3) a B&K Type 2610 measuring amplifier and a dual variable filter Kemo VBF 10M filter and (4) a B&K Type 2708 power amplifier to drive the underwater speaker. In addition, the experiment operators were able to hear and control the quality and the stability of the sound produced by the underwater speaker using a stereo amplifier and headset.

Laboratory data collection

Three different siphon conditions were simulated in the laboratory. They were as follows: (1) clean siphon with no damage, (2) siphon with variable amount of sediment and (3) siphon with six different artificial cuts. The sediment was simulated with acoustically transparent bags filled with fine sand. A maximum of 10 bags were used in this experiment, each bag weighted approximately 1 kg. The maximum cross-sectional dimension of one sandbag corresponded to approximately 20% of the pipe cross section. Several bags at a time were tied to a 9 m rope separated by a 300 mm distance, the number of bags deposited in the horizontal section of the siphon by these means varied from 1 to 10. Wall damages were created on the horizontal section of the siphon, the first type being a lateral cut of size 50 mm long. Its length was then increased to 100 and 200 mm to study the effect the extent of damage had on the quality of the pattern recognition algorithm. Another type of damage was a 55 mm longitudinal cut located at 1.5 m on the right of the lateral cut. The length of this type of cut was subsequently increased to 150 mm and was eventually converted into a 120 mm \times 70 mm hole. These conditions are illustrated in Figure 3(a)–(d).

Signal pre-processing

Acoustic impulse response

WinMLS software controlled the sound card which generated a 10 s sinusoidal sweep (chirp) in the frequency range of 100–6000 Hz. Sinusoidal sweep (chirp) is widely used excitation signal to measure the transfer function. Chirp-based measurements are considerably less vulnerable to the deleterious effect of time variance, and they are best suited for outdoor measurements in presence of dynamically rough water surface.¹⁷ The signal was repeated eight times and averaged to increase the signal-to-noise ratio. The sounds received on the four hydrophones were digitised at 22,050 Hz sampling rate and recorded on the PC.

Examples of the typical signal recorded in the clean siphon and in the siphon with two sandbags on the hydrophone array are given in Figure 4(a) and (b), respectively. Original acoustic signals received on hydrophones H1–H3 were de-convolved using the convolution theorem

$$h_l(t) = \text{Re}\{F^{-1}[F\{y_l(t)/F\{x(t)\}]\} \} \quad (1)$$

To obtain acoustic pressure response $h(t)$ at each of the three positions in the siphon where the hydrophones were installed. Here, $x(t)$ is the excitation signal, $y_l(t)$ is the signal recorded on the hydrophone l . It was assumed that the acoustic impulse response carries sufficient dynamic system information and can be used to study the characteristics of the system. However, the impulse response is a broadband acoustic signal and only a part of its spectrum is affected by the change in the siphon condition. A band-pass filter was used to study the effect of a change in the siphon condition on the acoustic impulse response. In this study, we adopted a third order Chebyshev Type 1 band-pass filter with

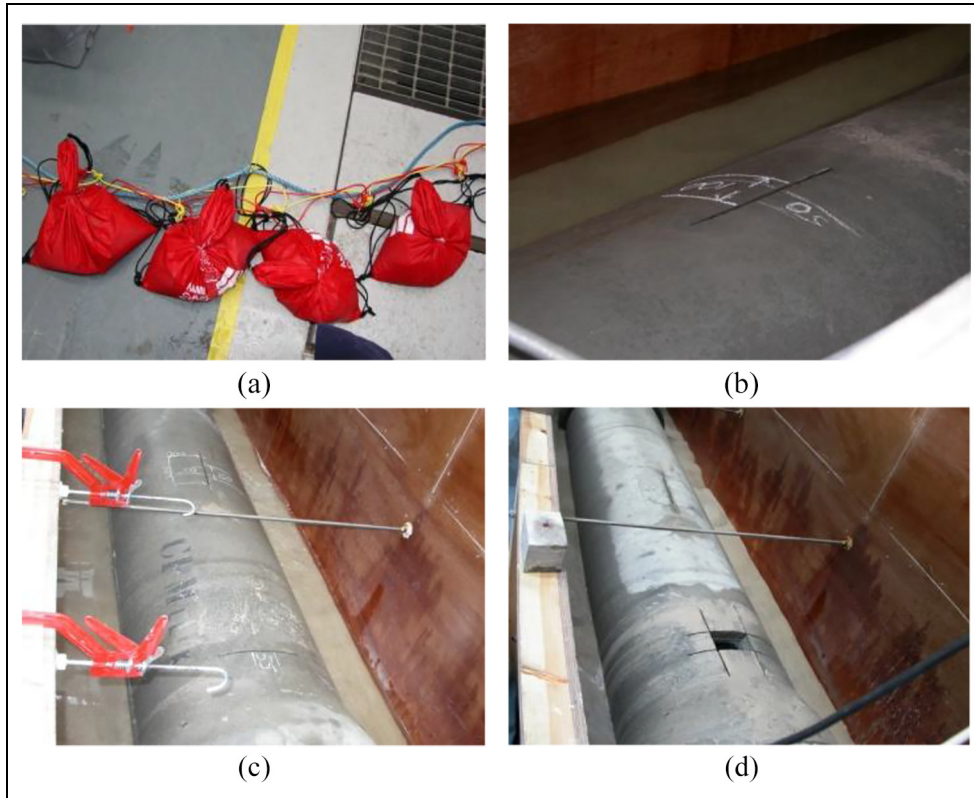


Figure 3. Siphon conditions simulated in the laboratory: Sandbags (a) and damages: lateral cut (b), longitudinal cuts (c) and manhole (d) on the pipe wall.

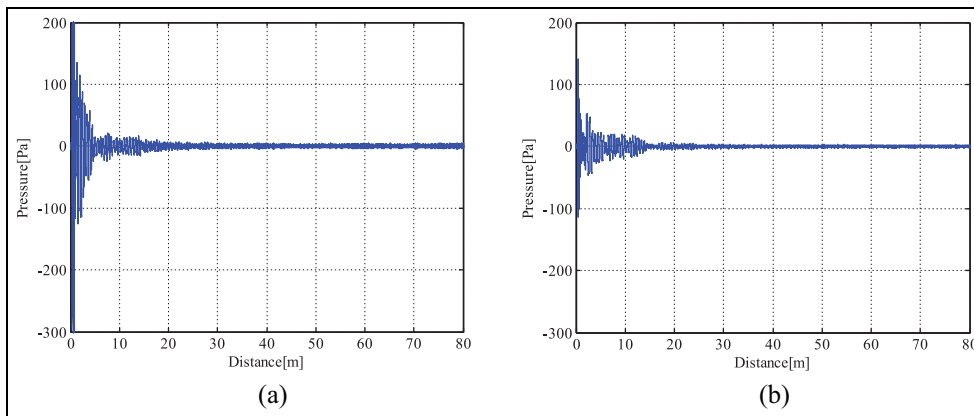


Figure 4. Acoustic pressure impulse response of clean siphon (a) and two sandbags in the siphon (b).

0.5 dB peak-to-peak ripple in the passband and 20 dB of stopband attenuation. This type of filter is frequently used in digital signal analysis and it provides a performance similar to that expected from a Butterworth filter at both low and high frequencies.¹⁸

The signals recorded on the three hydrophones were filtered in five filter bands. In the case of the blockage condition, these five 600 Hz bands split equidistantly in

the 100–3000 Hz frequency range. It was found that the sound pressure did not depend on the amount of blockage beyond 3000 Hz. In the case of the siphon with damage, the recorded signals were filtered in five 1000 Hz bands in the 100–5000 Hz frequency range. In this case, the sound pressure was found to be relatively insensitive to a change in the amount of damage at frequencies above 5000 Hz.

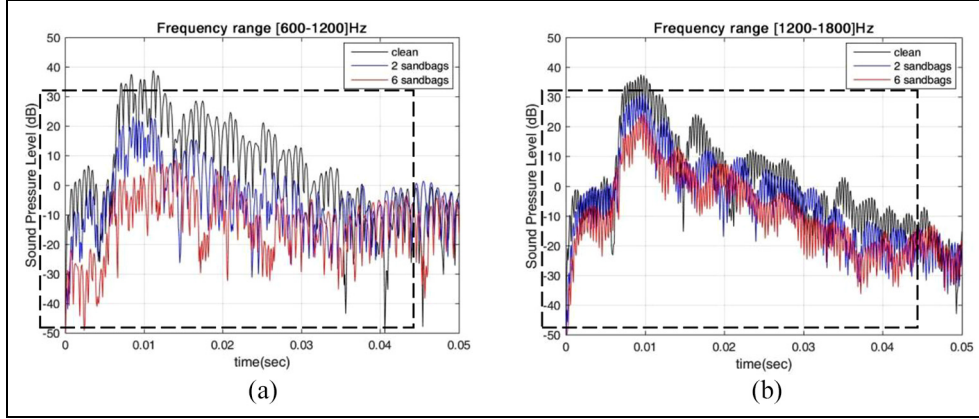


Figure 5. Sound pressure level of clean siphon, two sandbags and six sandbags in the siphon at frequency band 600–1200 Hz (a) and 1200–1800 Hz (b).

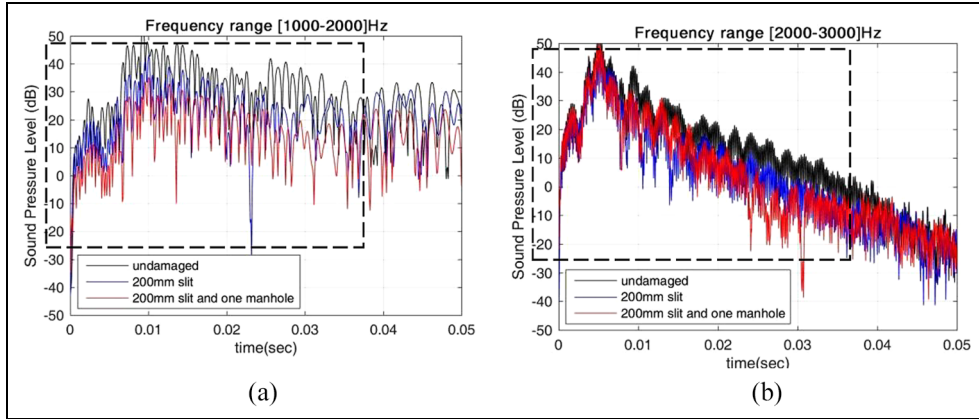


Figure 6. Sound pressure level of undamaged siphon, 200 mm slit and 200 mm slit + 1 manhole on the pipe wall at frequency band 1000–2000 Hz (a) and 2000–3000 Hz (b).

Sound pressure level

The impulse response obtained from equation (1) was then used to determine the sound pressure level as a function of time according to the Schroeder integral¹⁸

$$L(t) = 10 \log_{10} \left(\frac{1}{\Delta} \int_t^{t+\Delta} \hat{h}^2(t) dt \right) \quad (2)$$

where t is a time instant at which the sound pressure level is calculated, Δ is the duration of the integrating time interval and $\hat{h}(t)$ is the impulse response obtained on hydrophone l and filtered in the frequency band k . Figure 5 presents examples of the sound pressure level data calculated using the impulse response recorded on hydrophone 1 in the absence (1) and presence of two sandbags in the siphon filtered (2) in two frequency bands. Figure 6 is the sound pressure level of an undamaged siphon (1) and damaged siphon with a 120 mm \times 70 mm hole on the pipe wall (2) at two frequency

bands. However, it is not sufficient to determine the siphon conditions from the difference suggested in those figures. Hence, it is necessary to distract more characteristic information from sound pressure level data for the use of condition recognition process.

Feature extraction

Energy calculation

The feature extraction process was based on the estimation of the acoustic energy in the impulse response at a given instant. The acoustic energy¹⁹ was calculated as

$$E_{jkl} = \int_{t_j}^{t_j + \rho} 10^{L_{kl}(t)/10} dt \quad (3)$$

where the times t_j and $t_j + \rho$ define the time window j , within which the integration was carried out. The time

Table 1. The acoustic energy as a function of time and amount of porous sediment measured in the frequency band of 100–600 Hz.

Relative energy	t_1	t_2	t_3	t_4	t_5	t_6
Class 1 (clean pipe)	1.1487	2.1126	3.7360	5.5340	2.5631	0.9781
Class 2 (1 bag)	0.0652	0.2332	0.7196	1.2489	0.9794	0.6126
Class 3 (2 bags)	0.0153	0.0597	0.1622	0.7183	1.1071	0.6404
Class 4 (3 bags)	0.0078	0.0345	0.0966	0.5847	1.0419	0.4872
Class 5 (4 bags)	0.0208	0.0230	0.0871	0.3608	0.3474	0.1836
Class 6 (5 bags)	0.0117	0.0051	0.0513	0.2403	0.2890	0.0524
Class 7 (6 bags)	0.0114	0.0154	0.0436	0.1220	0.0926	0.1648
Class 8 (7 bags)	0.0082	0.0123	0.0226	0.0393	0.0284	0.3188
Class 9 (8 bags)	0.0004	0.0032	0.0087	0.0077	0.0692	0.1674
Class 10 (9 bags)	0.0003	0.0023	0.0039	0.0053	0.0312	0.0303
Class 11 (10 bags)	0.0003	0.0015	0.0044	0.0080	0.0188	0.0075

window used in this analysis was split in six equidistantly spaced time intervals of the width ρ . The width of the time window was selected empirically to ensure that the behaviour of the calculated acoustic energy reflects the decay rate in the impulse at which this energy was dissipated. In the case of a blockage condition, the time window was $0 \leq t \leq 45$ ms so that the interval width was $\rho = 7.5$ msec. In the case of a damaged condition, the time window was $0 \leq t \leq 36$ msec so that $\rho = 6$ msec.

Data tensor construction

Training data used in this work relate to a set of meaningful features that reflected the behaviour of the acoustic energy. These data were extracted from the acoustic signals collected from a range of known siphon conditions and used to provide criteria to compare against new data. The new data, or testing data, were collected from unknown siphon conditions. These data were used to study the performance of the classification algorithm, which was based on the KNN algorithm. The acoustic energy calculated for a range of known conditions was used to construct a four-dimensional (4D) training data table or 4D tensor \mathbf{E} , each element in this tensor is the value of the acoustic energy determined by the siphon condition (i), time window (j), frequency band (k) and hydrophone channel (l)

$$\mathbf{E} = \{E_{ijkl}\} \quad (4)$$

Table 1 presents an example of such data set for a range of blockage conditions. This table was constructed using the impulse response recorded on hydrophone 1 for 11 blockage conditions which are listed in the form of 11 rows and 6 columns (time windows). One particular frequency band (100–600 Hz) was used in the analysis. These data can be organised in the form of the following energy matrix $\mathbf{E} = \{E_{ij}\}$ where $i = 1, \dots, 11$ and $j = 1, \dots, 6$.

The acoustic energy training data matrix in Table 1 clearly illustrates that increasing the amount of porous sediment in the siphon results in a noticeable decrease in the calculated acoustic energy in all of the six time intervals. This decrease is particularly dramatic as the condition changes from one to four sandbags. A clear pattern in the behaviour of the acoustic energy as a function of the time interval can also be observed. The acoustic energy measured in the time interval $t_2 \leq t \leq t_5$ is generally higher than in the other intervals. Each element of this tensor is the value of the acoustic energy determined by siphon condition (i), time window (j), frequency band (k) and hydrophone (l). The rank of this tensor can be reduced to two dimensions (2D) or three dimensions (3D) if the signal is filtered in one frequency band and/or if the data from one hydrophone only are used in the analysis.

The damage condition training data tensor was created in the same manner. The elements in this tensor are the acoustic energies calculated using a different data set obtained independently in an experiment when controlled damage was inflicted to the siphon. The 4D of this tensor here correspond to the number of siphon damage conditions, six time windows, five frequency bands and three hydrophone channels. Table 2 presents an example of the damage condition training data matrix which was constructed using the signal recorded on hydrophone 1 and filtered in the frequency range of 100–1000 Hz.

Testing data were used to extract features from signals collected from unknown siphon conditions. Each of these data sets was organised in the form of a tensor using the procedure similar to that discussed in the previous paragraph. We used five sets of testing data recorded in the siphon with a blockage and five sets of data recorded in the siphon with some damage. For each unknown condition, a $1 \times 6 \times 5$ testing data energy matrix was constructed with one unknown siphon condition, six time windows and five frequency bands for one particular hydrophone.

Table 2. The acoustic energy as a function of time and amount of porous sediment measured in the frequency band of 100–1000 Hz.

Relative energy	t_1	t_2	t_3	t_4	t_5	t_6
Class 1 (undamaged pipe)	0.0228	1.9648	0.4031	0.0839	0.0537	0.0360
Class 2 (50 mm cut)	0.0679	3.0519	1.1786	0.1822	0.3956	0.0790
Class 3 (100 mm cut)	0.0600	3.3235	0.9099	0.3542	0.6084	0.1222
Class 4 (200 mm cut)	0.0063	0.2887	0.1280	0.0360	0.0211	0.0133
Class 5 (200 and 55 mm cut)	0.0084	0.5309	0.3197	0.1411	0.0356	0.0195
Class 6 (200 and 150 mm cut)	0.0084	0.5310	0.1576	0.0291	0.0203	0.0190
Class 7 (200 mm and square hole)	0.0108	1.2852	0.3392	0.0774	0.1887	0.0499

Condition classification

KNN algorithm

KNN is a commonly used classification method which is based on the use of distance measures.¹³ Given an unlabelled test data \mathbf{x} , find \mathbf{K} number of its ‘closest’ neighbours in a set of labelled training data $\{y_1, y_2 \dots y_n\}$ and assign \mathbf{x} to the label which appears most frequently within this particular data subset. Usually the Euclidean distance is used to determine the difference between the training energy data recorded for condition i and testing energy data for the condition which needs to be classified. This difference can be determined as

$$d_{jkl}(i) = |E_{ijkl} - X_{jkl}| \quad (5)$$

where X_{jkl} is a 3D tensor with the test data. In this work, the elements of this tensor are the acoustic energies calculated for the acoustic signal recorded on hydrophone l , filtered in the frequency band k and integrated in the time window j . The problem of condition classification can then be reduced to finding the minimum of $d_{jkl}(i)$ with respect to the condition index i , that is

$$\mathfrak{R}_{jkl} = \left\{ i : \min_i d_{jkl}(i) \right\} \quad (6)$$

where the 3D condition number tensor \mathfrak{R} is composed of the elements corresponding to one of the known siphon conditions as defined in the training data tensor \mathbf{E} . It is then possible to apply a majority vote to \mathfrak{R} in order to count the number of instances when a particular class (condition) along any of the 3D j, k, l appeared the most. This condition index can then be assigned as the condition (in the KNN sense) in which the siphon was at the time when the testing data were collected.

In general, \mathfrak{R} is defined to be a 3D tensor of size $J \times K \times L$, where J is the number of time windows used in the data analysis, K is the number of frequency bands and L is the number of hydrophones through which the

data were collected. However, the number of dimensions in \mathfrak{R} can be reduced if only one hydrophone channel is adopted or if the signal used in equation (3) is unfiltered or filtered in one frequency band only. In this case, \mathfrak{R} can be expressed in the matrix form (2D case) or as a data vector (one-dimensional (1D) case).

Decision making

Majority vote is a decision rule used in KNN classification method that normally select the number appearing more than half out of all numbers,¹³ but if there are more than two classes that the numbers can be divided among, then the number which has the highest times of appearance would make it the majority vote. The majority rule can stand even if there is only one more appearance for this number.

This section presents the majority vote which was applied progressively to 1D, 2D and 3D condition number tensor (\mathfrak{R}). The 1D condition number vector was constructed using the original unfiltered acoustical data recorded on hydrophone 1. The 2D condition matrix was constructed using the acoustical data recorded on hydrophone 1 and filtered in K frequency bands. The 3D condition number tensor was constructed using the acoustical data recorded on L hydrophones and filtered in K frequency bands. The majority votes were applied using condition numbers which were arranged in the form of a tensor \mathfrak{R} whose dimension was changed from one to three using the procedure outlined above. Examples of condition number tensors \mathfrak{R} for the blockage test and damage test data corresponding to three different types of analysis are shown in Table 3.

Majority vote was applied to each row of \mathfrak{R} constructed for the blockage and damage conditions in 1D, 2D and 3D. Some results obtained from this analysis are shown in Table 3. Four outcomes of the majority vote analysis were achieved: (1) the correct result, whereby the majority vote identified the correct condition in the siphon; (2) a false result, whereby the majority vote identified a wrong condition in the siphon; (3)

Table 3. Example applications of the majority vote analysis to blockage and damage test data.

Pipe condition \mathfrak{R} : (decision)	Test I (clean pipe) (class no.1)	Test I (undamaged pipe) (class no.1)
1D (time)	$(1 \quad 1 \quad 2 \quad 1 \quad 1 \quad 1) : (1)$	$(1 \quad 1 \quad 1 \quad 1 \quad 1 \quad 1) : (1)$
2D (time, frequency)	$\begin{pmatrix} 1 & 1 & 1 & 2 & 1 & 1 \\ 1 & 1 & 1 & 1 & 1 & 3 \\ 1 & 1 & 1 & 1 & 1 & 1 \\ 1 & 1 & 1 & 1 & 1 & 1 \\ 1 & 2 & 1 & 3 & 3 & 1 \end{pmatrix} : \begin{pmatrix} 1 \\ 1 \\ 1 \\ 1 \\ 1 \end{pmatrix} : (1)$	$\begin{pmatrix} 1 & 1 & 1 & 1 & 1 & 1 \\ 6 & 3 & 1 & 1 & 2 & 7 \\ 1 & 1 & 1 & 1 & 1 & 1 \\ 2 & 1 & 1 & 1 & 1 & 2 \\ 1 & 1 & 1 & 7 & 1 & 1 \end{pmatrix} : \begin{pmatrix} 1 \\ 1 \\ 1 \\ 1 \\ 1 \end{pmatrix} : (1)$
3D (time, frequency, hydrophone)	$\begin{pmatrix} 1 & 1 & 1 & 2 & 1 & 1 \\ 1 & 1 & 1 & 1 & 1 & 3 \\ 1 & 1 & 1 & 1 & 1 & 1 \\ 1 & 1 & 1 & 1 & 1 & 1 \\ 1 & 2 & 1 & 3 & 3 & 1 \\ \hline 1 & 1 & 2 & 2 & 3 & 1 \\ 1 & 1 & 1 & 1 & 1 & 3 \\ 1 & 1 & 1 & 1 & 1 & 1 \\ 1 & 1 & 1 & 1 & 8 & 1 \\ 1 & 3 & 1 & 4 & 4 & 1 \\ \hline 1 & 1 & 2 & 2 & 3 & 1 \\ 1 & 1 & 1 & 1 & 1 & 1 \\ 1 & 1 & 1 & 1 & 1 & 1 \\ 1 & 1 & 1 & 1 & 1 & 1 \\ 1 & 1 & 2 & 4 & 4 & 3 \end{pmatrix} : \begin{pmatrix} 1 \\ 1 \\ 1 \\ 1 \\ 1 \\ 1 \\ 1 \\ 1 \\ 1 \\ 1 \\ 1 \\ 1 \\ 1 \\ 1 \\ 1 \\ 1 \end{pmatrix} : (1)$	$\begin{pmatrix} 1 & 1 & 1 & 1 & 1 & 1 \\ 6 & 3 & 1 & 1 & 2 & 7 \\ 1 & 1 & 1 & 1 & 1 & 1 \\ 2 & 1 & 1 & 1 & 1 & 2 \\ 1 & 1 & 1 & 7 & 1 & 1 \\ \hline 1 & 1 & 1 & 1 & 1 & 1 \\ 5 & 2 & 1 & 1 & 7 & 7 \\ 7 & 1 & 1 & 6 & 1 & 7 \\ 1 & 1 & 1 & 1 & 4 & 1 \\ 1 & 1 & 1 & 1 & 1 & 1 \\ \hline 1 & 1 & 1 & 1 & 2 & 1 \\ 5 & 1 & 1 & 1 & 7 & 7 \\ 1 & 1 & 7 & 1 & 1 & 1 \\ 1 & 1 & 1 & 1 & 1 & 1 \\ 1 & 1 & 1 & 7 & 1 & 1 \end{pmatrix} : \begin{pmatrix} 1 \\ 1 \\ 1 \\ 1 \\ 1 \\ 1 \\ 1 \\ 1 \\ 1 \\ 1 \\ 1 \\ 1 \\ 1 \\ 1 \\ 1 \\ 1 \end{pmatrix} : (1)$

1D: one dimension; 2D: two dimensions; 3D: three dimensions.
 *A stands for 'ambiguous result', that is, when no certain decision can be made based on MV.

an ambiguous result, when no clear decision could be drawn from majority vote because the correct condition number appeared as frequent as another condition number; and (iv) a failure to make a decision as all condition numbers appeared equal times. In the case of 1D data, the majority vote was simply based on the highest times of appearance of one particular condition in the index vector as illustrated in the first row of Table 3. In the case of 2D data, the majority vote rule was initially applied row-wise so that the index matrix \mathfrak{R} was reduced to an index column. The majority vote rule was then applied again to the resultant index column as it was done in the 1D case. This process is illustrated in the second row of Table 3. In the case of 3D data, the majority vote rule was applied three times so that the rank of the 3D index tensor \mathfrak{R} was gradually reduced until the final classification was made. This is illustrated in the third row of Table 3.

The probability distribution was also calculated for 2D and 3D condition numbers using the following equation

$$\Pr(X = \mu|N) = \frac{N_{\mu}}{N}, \sum_{\mu=1}^I \Pr(X = \mu) = 1 \quad (7)$$

where N is the number of all condition estimations and N_{μ} is the number of condition estimation, X chosen to be class $\mu, \mu \in [1, I], I$ is the maximum number of siphon conditions.

The statistical probability for the correct classification was calculated as the proportion of the correct classification instances observed in the 3D index tensor \mathfrak{R} and as the proportion of the correct majority votes. The results are shown in Table 4. In the case of the blockage tests, the results of majority vote applied to 1D unfiltered data for some siphon conditions are either ambiguous or incorrect. Here, the probability of the correct estimation determined from the condition number vector \mathfrak{R} is generally below 50%. The 2D and 3D classification results show higher certainty due to the filtering of acoustic signals in several narrow lower frequency bands which contain less ambiguous information about the siphon conditions than those confined to the higher frequency bands. The probability

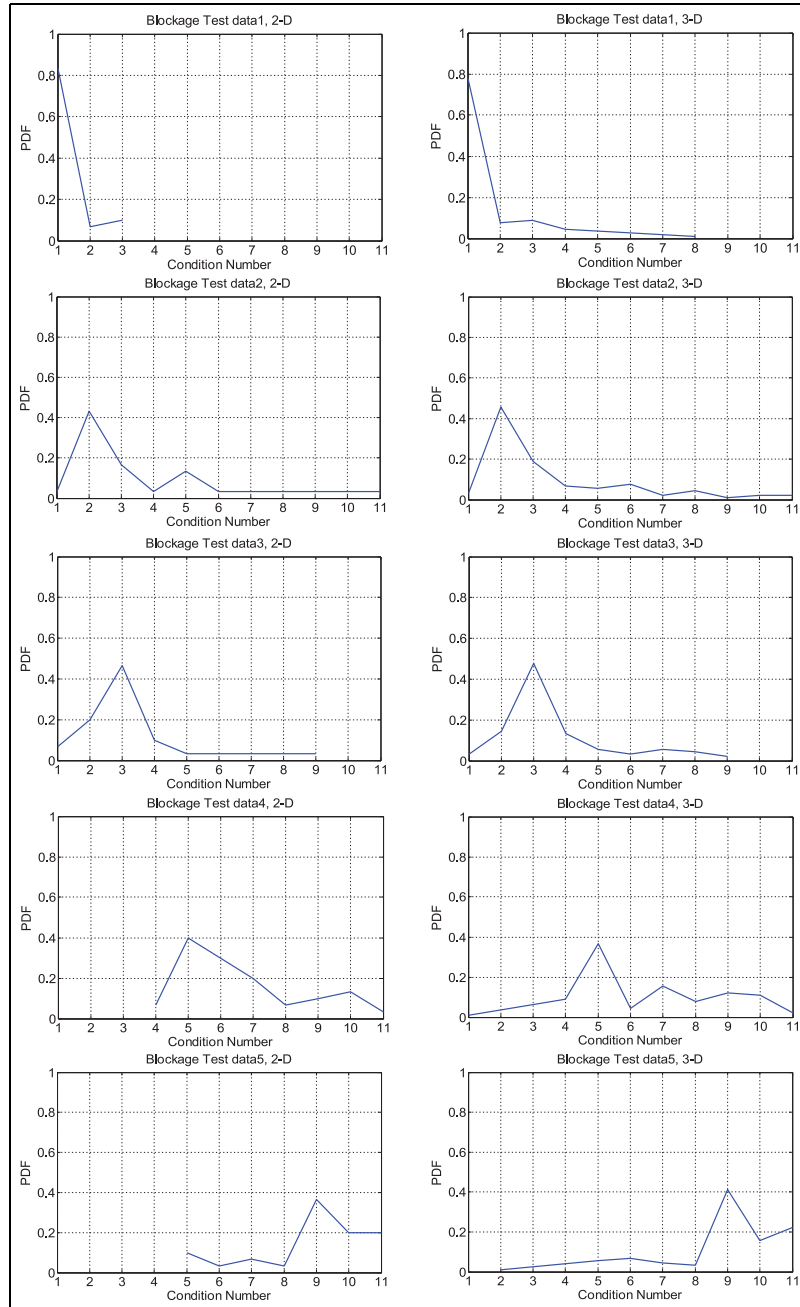


Figure 7. The probability density functions for the blockage condition estimation based on five sets of test data: 2D (left) and 3D (right).

Table 4. Proportion of the correct condition estimations from the index tensor \mathfrak{R} .

Number of correct condition estimations/ all estimations	Blockage		Damage	
	\mathfrak{R}	MV	\mathfrak{R}	MV
1D	46.7%	60%	90.0%	100%
2D	50.0%	72%	77.3%	96%
3D	49.8%	76%	73.1%	88%

MV: majority vote; 1D: one dimension; 2D: two dimensions; 3D: three dimensions.

for the correct classification in the majority vote experiment with a blockage was 60% for 1D analysis. This probability increased to 72% and 76% for 2D and 3D classification analysis, respectively.

The probability of the correct classification for the algorithm based on the 3D index tensor \mathfrak{R} is approximately 90%. These probabilities reduce slightly to 77% and 73% when the tensor dimensionality was increased to 2D and 3D, respectively (see Table 4). The majority vote analysis works better for the damage condition classification. Table 4 shows that the probability of the

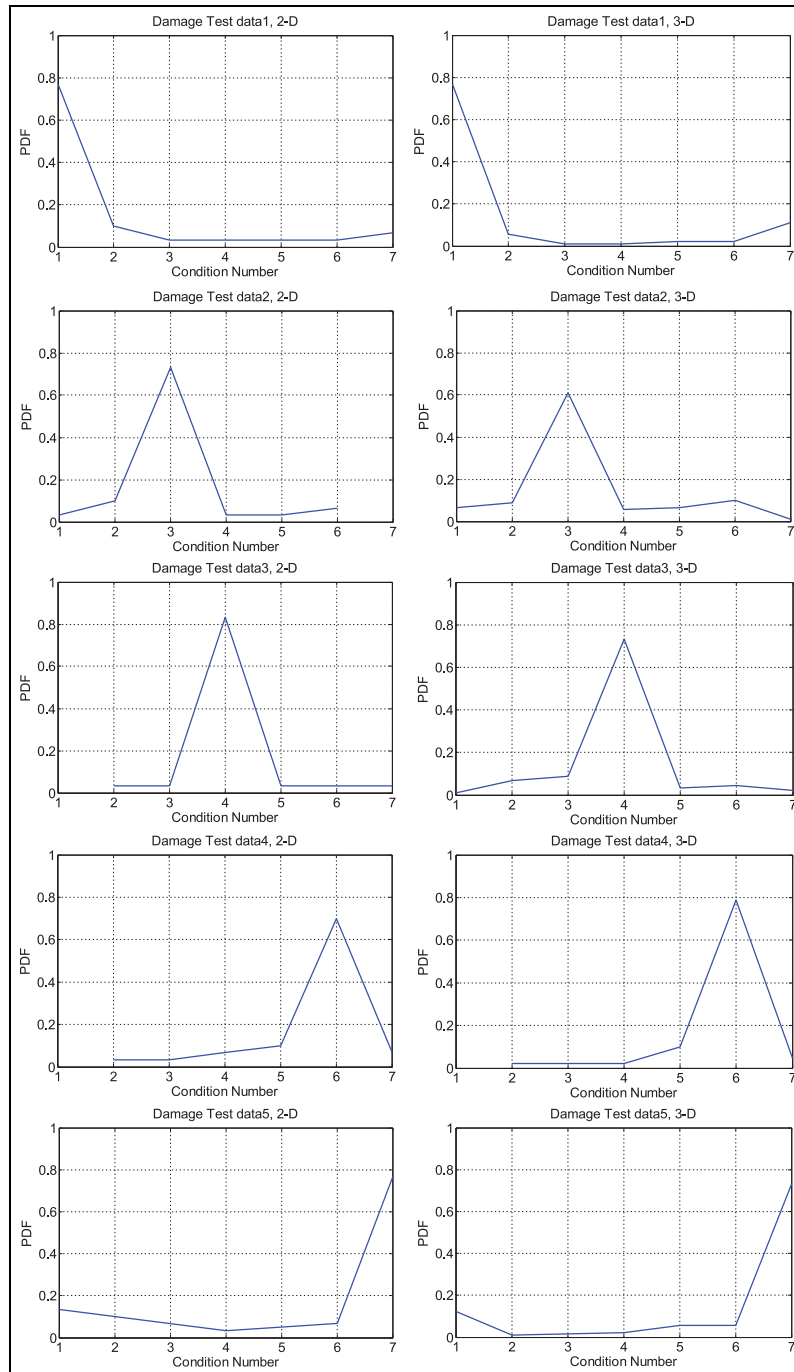


Figure 8. The probability density function for the damage condition estimation based on five sets of test data: 2D (left) and 3D (right).

correct classification with this method is 100% in the case of 1D analysis. This probability decreases slightly with the increased dimensionality of the problem (see Table 4).

Figures 7 and 8 present the probability as a function of the condition number of all five test data sets for the blockage and damage conditions, respectively. Each of these graphs shows a maximum which corresponds to

the condition number that occurs most often in the test data set. In the blockage experiment, the amplitude of this maximum tends to reduce with the increased amount of sediment deposited in the pipe. In the damage experiment, the amplitude of this maximum is relatively unaffected by the extent of the damage inflicted on the siphon. In both experiments, the maximum in

the probability data remained sufficiently distinct to be used for condition classification.

The results of damage classification are less ambiguous than the results of blockage classification. One explanation for this difference is that the positions of acoustic source and hydrophones were undisturbed when more damage was inflicted to the pipe. On the contrary, the position of the source and receive array were disturbed each time when more sediment was added to the siphon to simulate the blockage evolution. In this way, the recorded acoustic impulse response was affected in the blockage experiment. This phenomenon relates to the multi-modal nature of the sound field in the siphon and strong variations in the sound field as a function of the sensor position. It was noticed that using acoustic energy as a feature to discriminate between damaged siphon conditions by applying KNN algorithm and majority vote wisely can achieve more accurate results. The results of the 1D classification analysis suggest that unfiltered acoustic data can provide sufficient information to correctly identify various damage conditions.

Summary

Acoustic signals were collected from a range of typical blockage and damage siphon conditions which were recreated in the laboratory. The sound pressure level was calculated so that the acoustic energy as a function of time could be determined and used as a feature in the classification analysis. Original broadband signals recorded on hydrophone 1 were used for 1D analysis, and these signals were then filtered by Chebyshev type I digital filter in several narrow frequency bands and used in 2D analysis. More acoustic data recorded on hydrophones 2 and 3 were added to the analysis to make it 3D.

KNN was used as classification method to classify the siphon conditions. The acoustic technique and the adopted KNN classification system are proved to be capable of discriminating different siphon conditions collected under blockage and damage conditions were used to provide training and testing data for classification. For blockage conditions, acoustic data in the lower frequency bands contain more useful information than those filtered through the higher frequency bands. Therefore, 2D and 3D data analysis yielded better a classification than 1D data. Majority vote improved the performance of the classification algorithm by removing some uncertainty from the data. Damage classification results cannot be improved by increasing the number of the index tensor dimensions used in the analysis. This suggests that the acoustic energy calculated from data collected under damage conditions are less frequency dependent than in the blockage

condition case. The recorded acoustic impulse response is sensitive to the sensor position and this effect needs to be taken into account computationally or through improving the procedure for these experiments.

Acknowledgements

The author was very grateful to Professor K.V.H. from The University of Sheffield (UK) for constructing the experimental facility in the Hydraulics Laboratory at the University of Bradford (UK) and his supervision on this work.


Declaration of conflicting interests

The author(s) declared no potential conflicts of interest with respect to the research, authorship and/or publication of this article.

Funding

The author(s) disclosed receipt of the following financial support for the research, authorship and/or publication of this article: This research is supported by the National Natural Science Foundation of China (No. 61563024 and No. 61663017).

ORCID iD

Zao Feng  <https://orcid.org/0000-0002-9476-3978>

References

1. Liu Z and Kleiner Y. State of the art review of inspection technologies for condition assessment of water pipes. *Measurement* 2013; 46: 1–15.
2. Datta S and Sarkar S. A review on different pipeline fault detection methods. *J Loss Prevent Proc* 2016; 41: 97–106.
3. Davis P, Sullivan E, Marlow D, et al. A selection framework for infrastructure condition monitoring technologies in water and wastewater networks. *Expert Syst Appl* 2013; 40: 1947–1958.
4. Besancon G, Scola IR, Guillén M, et al. Observer-based detection and location of partial blockages in pipelines. In: *Conference on control and fault-tolerant systems*, Nice, 9–11 October 2013. New York: IEEE.
5. Bhuiyan MAS, Hossain MA and Alam JM. A computational model of thermal monitoring at a leakage in pipelines. *Int J Heat Mass Tran* 2016; 92: 330–338.
6. Muggleton JM, Brennan MJ and Gao Y. Determining the location of buried plastic water pipes from measurements of ground surface vibration. *J Appl Geophys* 2011; 75: 54–61.
7. Zhang C and Heidemann J. Accurate pipeline blockage detection with low-cost multi-modal sensing. In: *Proceedings of the 11th IEEE international conference on mobile ad hoc and sensor systems*, Philadelphia, PA, 28–30 October 2014. New York: IEEE.
8. Ergen E, Guven G, Kurc O, et al. Blockage assessment of buildings during emergency using multiple types of sensors. *Automat Constr* 2015; 49: 71–82.

9. Liu C-W, Li Y-X, Yan Y-K, et al. A new leak location method based on leakage acoustic waves for oil and gas pipelines. *J Loss Prevent Proc* 2015; 35: 236–246.
10. Duan HF, Lee PJ, Ghidaoui MS, et al. Transient wave-blockage interaction and extended blockage detection in elastic water pipelines. *J Fluid Struct* 2014; 46: 2–16.
11. Duan W, Kirby R, Prisutova J, et al. On the use of power reflection ratio and phase change to determine the geometry of a blockage in a pipe. *Appl Acoust* 2015; 87: 190–197.
12. Meseguer J, Puig V and Escobet T. Fault diagnosis using a timed discrete-event approach based on interval observers: application to sewer networks. *IEEE T Syst Man Cy A* 2010; 40: 900–916.
13. Kumar M, Jindal MK and Sharma RK. k -Nearest neighbor based offline handwritten Gurmukhi character recognition. In: *International conference on image information processing*, Shimla, India, 3–5 November 2011. New York: IEEE.
14. Qu Z, Wang H, An Y, et al. Online monitoring method of hydrate agglomeration in natural gas pipelines based on acoustic active excitation. *Measurement* 2016; 92: 11–18.
15. Yuan Z, Deng Z and Jiang M. Extended partial blockage detection in a gas pipeline based on Tikhonov regularization. *J Nat Gas Sci Eng* 2015; 27: 130–137.
16. Tolstoy A, Horoshenkov KV and Bin Ali MT. Detecting pipe changes via acoustic matched field processing. *Appl Acoust* 2009; 70: 695–702.
17. Holters M, Corbach T and Zölzer U. Impulse response measurement techniques and their applicability in the real world. In: *Proceedings of the 12th International Conference on Digital Audio Effects (DAFx-09)*, Como, Italy, 1–4 September 2009.
18. Rossing TD. *Handbook of acoustics*. New York: Springer Science + Business Media, 2007.
19. Fuller CR and Fahy FJ. Characteristics of wave propagation and energy distributions in cylindrical elastic shells filled with fluid. *J Sound Vib* 1982; 81: 501–518.